

FULLY 3D MULTIPLE BEAM DYNAMICS PROCESSES SIMULATION FOR THE TEVATRON

E. Stern*, J. Amundson, P. Spentzouris, CPA/CD, FNAL, Batavia, IL 60510, USA
A. Valishev, AD, FNAL, Batavia, IL, 60510, USA

Abstract

Extensive work has been done to create an accurate model of beam dynamics at the Fermilab Tevatron. This paper will present validation and results from the development of a simulation of the machine including multiple beam dynamics effects. The essential features of the simulation include a fully 3D strong-strong beam-beam particle-in-cell Poisson solver, interactions among multiple bunches and both head-on and long-range beam-beam collisions, coupled linear optics and helical trajectory consistent with beam orbit measurements, chromaticity and resistive wall impedance. The individual physical processes are validated against measured data where possible, and analytic calculations elsewhere. The simulation result discussion will focus on the effects of increasing beam intensity with single and multiple bunches on the impedance of the beams.

INTRODUCTION

The Fermilab Tevatron [1] is a $p\bar{p}$ collider operating at a center-of-mass energy of 1.96 TeV and peak luminosity reaching $3.15 \times 10^{32} \text{ cm}^{-2} \text{ s}^{-1}$. Each of the colliding beams consists of 36 bunches following a helical trajectory moving in a common vacuum pipe. Bunches from opposing beams pass each other at 138 interaction points (IPs) around the ring. During setup for high-energy physics operations, the beams influence each other through long-range beam-beam interactions at the crossing points. For high-energy physics operations, the beams are brought into head-on collision at just two interaction points (IPs) surrounded by particle detectors but the other 136 IPs remain as long-range (or parasitic) IPs. The combined effect of machine impedance and beam-beam interactions in extended length bunches couples longitudinal motion to transverse degrees of freedom and may produce a dipole or quadrupole mode instability [2]. The helical orbit of the beams and the bucket fill pattern in the machine means that each bunch experiences a different environment, and each bunch is coupled to all other bunches through beam-beam or impedance effects leading to the possibility of coherent modes. Effects arising from both head-on and long-range beam-beam interactions impose serious limitations on machine performance, hence constant efforts are being exerted to better understand the beam dynamics. Due to extreme complexity of the problem a numerical simulation appears to be one of the most reliable ways to study performance of the system.

We will present a comprehensive Tevatron simulation including a fully 3D strong-strong beam-beam particle-in-cell Poisson solver, interactions among multiple bunches with both head-on and long-range collisions, a linear optics model using measured coupled lattice functions, a helical trajectory consistent with beam-orbit measurements, and machine chromaticity and impedance. Finally, we will show some simulations of several different scenarios of machine intensity and discuss possible instabilities.

SIMULATION

The starting point for our simulations is the extended BeamBeam3d code described in references [3, 6]. Bunches of macro-particles in two beams are generated with a random distribution in phase space with parameters that match the lattice. The accelerator ring is conceptually divided into arcs with potential interaction points at the ends of the arcs. All bunches from both beams are individually tracked. When bunches from two beams arrive at the same IP, a Poisson field solver is employed to determine the electromagnetic forces on each particle produced by the charged particles in the opposing beam bunch. Beam-beam forces in extended length bunches are computed by slicing the bunch longitudinally and moving the bunches through other in steps, applying the beam-beam forces at each step.

The optics of each arc is modeled with a 6×6 linear map that transforms the phase space $\{x, x', y, y', z, \delta\}$ coordinates of each macroparticle from one end of the arc to the other. There is a significant amount of coupling between the horizontal and vertical transverse coordinates in the Tevatron. For our Tevatron simulations, the maps were calculated using coupled lattice functions [4] obtained by fitting a model [5] of beam element configuration to beam position measurements. The synchrotron motion is put in as a sinusoidal oscillation with the periodicity of the machine synchrotron tune. The Tevatron includes electrostatic separators to generate a helical trajectory for the oppositely charged beams. A shifted Greens function is employed in the Poisson field solver calculation to efficiently account for the mean beam transverse offset at each IP.

The validity of the 3D beam-beam calculation has been verified[6] by reproducing the evolution[7] of synchrotron modes observed at the VEPP-2M e^+e^- collider as a function of beam-beam parameter ξ .

Chromaticity results in an additional momentum dependent phase advance $\delta\mu_{x(y)} = \mu_0 C_{x(y)} \Delta p/p$ where $C_{x(y)}$ is the chromaticity for x (or y) and μ_0 is the design phase advance for the arc. The additional phase advance is ap-

* egstern@fnal.gov

plied to each particle in the decoupled coordinate basis so that symplecticity is preserved.

The impedance model applies a momentum kick to the particles generated by the dipole component of resistive wall wakefields [8]. Each beam bunch is divided longitudinally into slices containing approximately equal numbers of particles. As each bunch is transported through an arc, particles in slice i receive a transverse kick from the wake field induced by the dipole moment of the particles in forward slice j :

$$\frac{\Delta \vec{p}_\perp}{p} = \frac{2}{\pi b^3} \sqrt{\frac{4\pi\epsilon_0 c}{\sigma}} \frac{N_j r_p \langle \vec{r}_j \rangle}{\beta\gamma} \frac{L}{\sqrt{z_{ij}}} \quad (1)$$

The length of the arc is L , N_j is the number of particles in slice j , r_p is the classical electromagnetic radius $e^2/4\pi\epsilon_0 mc^2$, z_{ij} is the longitudinal distance between the particle in slice i that suffers the wakefield kick and slice j that induces the wake. \vec{r}_j is the mean transverse position of particles in slice j , b is the pipe radius, c is the speed of light, σ is the conductivity of the beam pipe and $\beta\gamma$ are Lorentz factors of the beam, and quantities with units are specified in the MKSA system.

The impedance model has been verified to agree with analytic calculations of instability thresholds and growth rates for the two macroparticle model of strong and weak head-tail instabilities[6, 8].

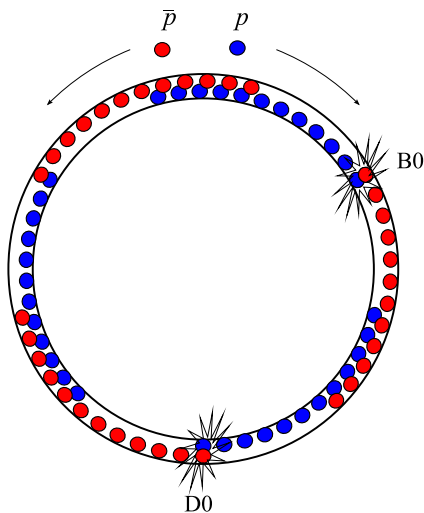


Figure 1: Schematic of proton (blue) and antiproton (red) bunches in the Tevatron and the two head-on collision locations B0 and D0.

EMITTANCE GROWTH

The fill pattern of bunches in the Tevatron for protons and antiprotons consists of three trains of twelve bunches each as indicated schematically in Fig. 1. Bunches collide head-on at the B0 and D0 interaction points but undergo long range (electromagnetic) beam-beam interactions at

Beam Dynamics and Electromagnetic Fields

D05 - Code Developments and Simulation Techniques

136 other locations around the ring. The long-range collision locations that are closest to main head-on collision IP have a beam separation of about six beam σ . The two beams are separated by at least eight beam σ at all other long-range collision locations and their beam-beam effects would be attenuated by the inverse square. Running the simulation with all 136 long-range IPs turns out to be very slow so we only calculated beam-beam forces at the two main IPs and the long-range IPs immediately upstream and downstream of them. In addition, the transverse beta functions at the long-range collision locations are much larger than the bunch length, so the beam-beam calculation at those locations can be performed using only the 2D solver.

One interesting consequence of the fill pattern and the helical trajectory is that any one of the 12 bunches in a train experiences collisions with the 36 bunches in the other beam at different locations around the ring, and in a different transverse position. This results in a different tune and emittance growth for each bunch of a train, but with the three-fold symmetry for the three trains. This is observed experimentally[9].

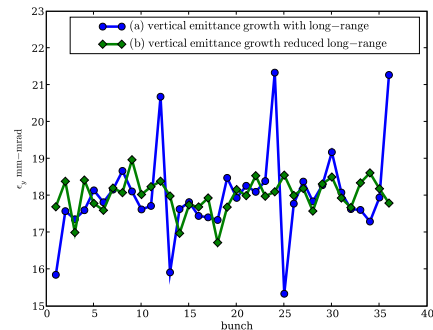


Figure 2: The vertical emittance of each bunch in a 50000 turn simulation of 36 proton on 36 antiproton bunches in the Tevatron. Curve (a) simulates normal operating conditions with the nominal beam spacing at the long-range IPs. Curve (b) simulates the hypothetical condition with the beam separation at the long-range IPs is 100 times normal, eliminating the the effect of those long-range IPs.

The beam-beam simulation with 36-on-36 bunches shows similar effects. We ran a simulation of 36 proton on 36 antiproton bunches for 50000 turns with the nominal helical orbit. The proton bunches had 8.8×10^{11} particles (roughly four times the usual to enhance the effect) and The proton emittance was the the typical 20π mm-mrad. The antiproton bunch intensity and emittance were both half the corresponding proton bunch parameter. The initial emittance for each proton bunch was the same so changes during the simulation reflect the beam-beam effect.

Curve (a) in Figure 2 shows the vertical emittance for each of the 36 proton bunches in a 36-on-36 simulation after 50000 turns of simulation. The three-fold symmetry is evident. The end bunches of the train are clearly different

from the interior bunches. For comparison, Fig. 3 shows the measured vertical emittance taken during accelerator operations.

The bunches in the interior of each train have two long-range collisions at an long-range IP closest to the head-on IP; one before and one after. In contrast, the bunch at the end of the train only has one long-range collision at a close IP. To test whether this is the origin of the bunch difference, we performed another simulation, but with beam separation at the closest head-on IP expanded 100 times it's nominal value resulting in Figure 2 curve (b) showing a much reduced bunch-to-bunch variation. We conclude that the beam-beam effect at the long-range IPs is the origin of a large part of the bunch variation.

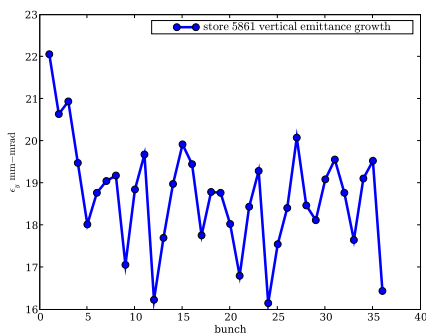


Figure 3: The measured vertical emittance after 15 minutes of a particular store (#5861) of particles in the Tevatron, showing an emittance growth pattern similar to the simulation results in Figure 2.

OPERATIONAL INSTABILITIES

With proton bunch intensities currently approaching 3.0×10^{11} particles, the chromaticity of the Tevatron has to be managed carefully to avoid the development of a head-tail instability. Running with positive chromaticities is well known to suppress the head-tail instability but leads to larger beam losses which can damage accelerator and experimental apparatus, so an effort is underway to determine a safe lower limit for chromaticity. Our multi-physics simulation can be part of this investigation.

Initially in the injection process, the chromaticity of the ring is kept high to damp the head-tail instability, and the proton and antiproton beams are kept apart with electrostatic separators. After the beams are brought into collision at the main IPs, the chromaticity is reduced. With a large enough beam-beam effect, Landau damping will control the head-tail instability [10]. The concern is that before the beams are brought into collision, there might be insufficient beam-beam effect to damp the instability.

Our simulations were performed with starting beam parameters listed in Table 1, varying chromaticity. With chromaticity set to -2 units, and no beam-beam effect, the beams are clearly unstable as seen in Fig. 4. With beams

Table 1: Beam parameters for Tevatron simulation

Parameter	value
beam energy	980 GeV
p particles/bunch	3.0×10^{11}
\bar{p} particles/bunch	0.9×10^{11}
p tune (Q_x, Q_y)	(20.585, 20.587)
p (normalized) emittance	20π mm-mrad
\bar{p} tune (Q_x, Q_y)	(20.577, 20.570)
\bar{p} (normalized) emittance	6π mm-mrad
synchrotron tune Q_s	0.0007
slip factor	0.002483
bunch length (rms)	43 cm
$\delta p/P$ momentum spread	1.2×10^{-4}
effective pipe radius	3 cm

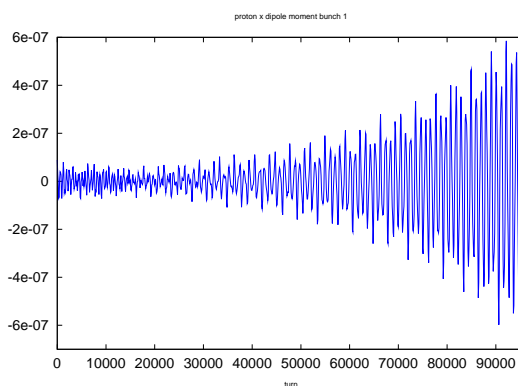


Figure 4: The x dipole moment in a simulation with $C = -2$ no beam-beam effect showing instability.

separated, turning on the beam-beam effect prevents rapid oscillation growth during the simulation (Fig. 5). The sudden bursts of increased amplitude is sometimes indicative of the onset of instability, but it is not obvious within the limited duration of this run. Interestingly, the RMS size of the beam is also growing as shown in Fig. 6.

The dipole moment from simulation with positive chromaticity shown in Fig. 7 does not look markedly different than the negative chromaticity simulation, but the RMS moment shown in Fig. 8) shows a much smaller RMS growth.

Another question is if we are relying on beam-beam effects to stabilize the the beam, can we see a difference in stability by increasing the antiproton beam strength in the marginally stable case of $C = -2$? Fig. 9 shows the dipole motion of a representative bunch in a simulation with $C = -2$, but twice the number of antiprotons (the emittance is also doubled). Again, as with Fig. 5, there is no obvious instability, but the beam size indicated by the RMS shown in Fig. 10 exhibits very little growth compared with Fig. 6, even taking into account that the run was only 30000 turns instead of 40000. This suggests that both head-tail instability and growth in beam size should be consid-

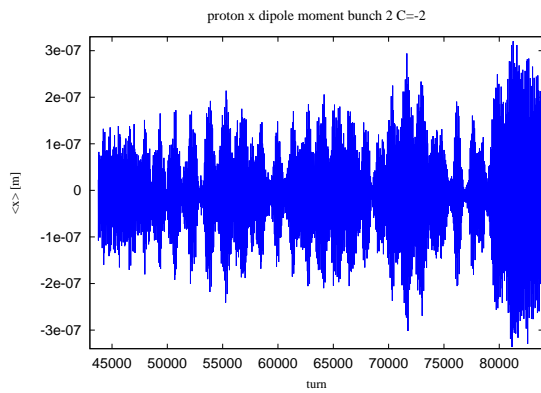


Figure 5: The x dipole moment of a representative bunch in a 36-on-36 simulation with $C = -2$ with beam-beam effects and beams separated showing no obvious instability within the limits of the simulation.

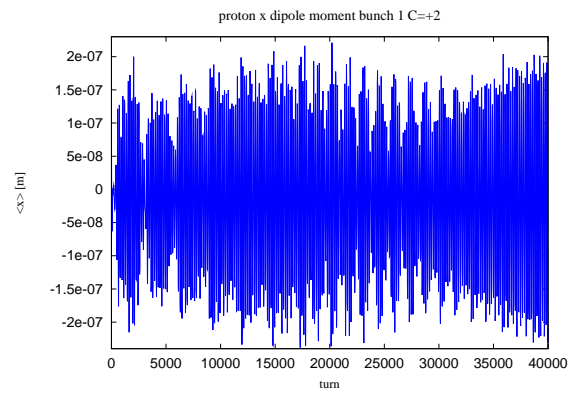


Figure 7: The x dipole moment in a simulation with $C = +2$ with beam-beam effects and beams separated showing no obvious instability.

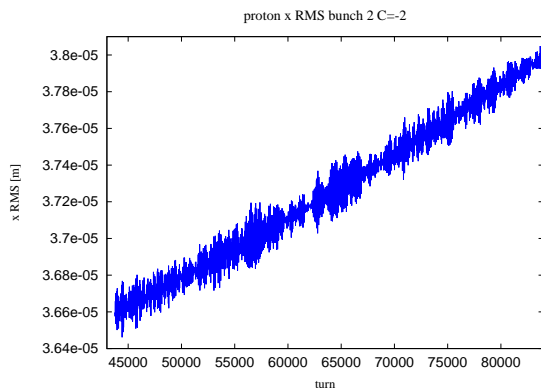


Figure 6: The x bunch RMS in a simulation with $C = -2$ with beam-beam effects and beams separated showing beam-spot growth.

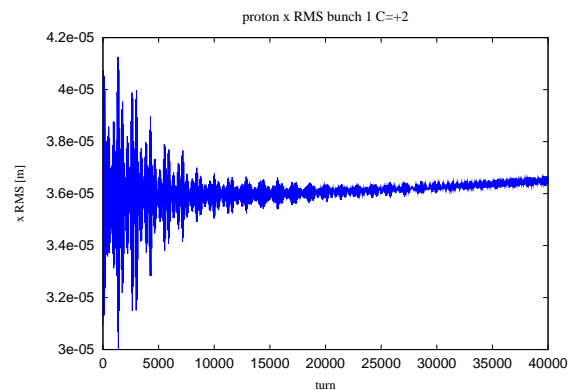


Figure 8: The x position RMS in a simulation with $C = +2$ with beam-beam effects and beams separated showing reduced beam RMS growth compared with the $C = -2$ case.

ered in machine operation with lower levels of antiprotons in the machine and separated beams.

CONCLUSIONS

The comprehensive simulation of the Tevatron including measured machine optics and beam orbits, beam-beam effects, chromaticity, resistive wall impedance, and multiple bunch tracking reproduces observed idiosyncratic Tevatron behavior. Simulations of different operating conditions can guide machine physicists in planning operating parameters and understanding the complicated interaction of multiple effects. The execution time of the simulations should be improved so that they can address issues faster with more completeness.

ACKNOWLEDGEMENTS

We thank J. Qiang and R. Ryne of LBNL for the use of and assistance with the BeamBeam3d program. This work was supported by the United States Department

of Energy under contract DE-AC02-07CH11359 and the COMPASS project funded through the Scientific Discovery through Advanced Computing program in the DOE Office of High Energy Physics. This research used resources of the National Energy Research Scientific Computing Center, which is supported by the Office of Science of the U.S. Department of Energy under Contract No. DE-AC02-05CH11231. This research used resources of the Argonne Leadership Computing Facility at Argonne National Laboratory, which is supported by the Office of Science of the U.S. Department of Energy under contract DE-AC02-06CH11357.

REFERENCES

- [1] Run II handbook, <http://www-bd.fnal.gov/runII>.
- [2] E.A. Perevedentsev and A.A. Valishev, "Simulation of Head-Tail Instability of Colliding Bunches", Phys. Rev. ST Accel. Beams **4**, 024403, (2001).
- [3] J. Qiang, M.A. Furman, R.D. Ryne, J.Comp.Phys., 198

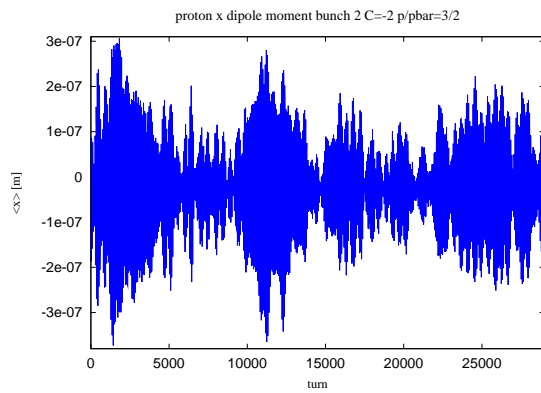


Figure 9: The x dipole moment of a representative bunch in a 36-on-36 simulation with $C = -2$, beam-beam effects and antiproton beam intensity doubled compared to run shown in Fig. 5.

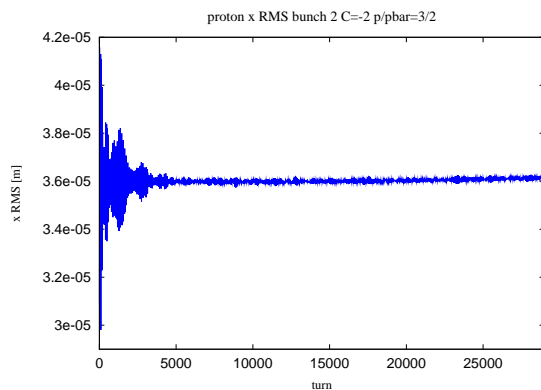


Figure 10: The x bunch RMS in a simulation with $C = -2$, beam-beam effects and antiproton beam intensity doubled compared to the run shown in Fig. 6. The growth rate is markedly reduced.

(2004), pp. 278–294, J. Qiang, M.A. Furman, R.D. Ryne, Phys. Rev. ST Accel. Beams, 104402 (2002).

- [4] V. Lebedev, <http://www-bdnew.fnal.gov/pbar/organizationalchart/lebedev/OptiM/optim.htm>.
- [5] A. Valishev *et al.*, “Progress with Collision Optics of the Fermilab Tevatron Collider”, EPAC06, Edinburgh, Scotland, 2006.
- [6] E. Stern *et al.*, “Development of 3D Beam-Beam Simulation for the Tevatron,” TUODC02, PAC07, Albuquerque, NM, USA, 2007.
- [7] I.N. Nesterenko, E.A. Perevedentsev, A.A. Valishev, Phys.Rev.E, 65, 056502 (2002).
- [8] A. Chao, *Physics of Collective Beam Instabilities in High Energy Accelerators.*, pp. 56–60, 178–187, 333–360 John Wiley and Sons, Inc., (1993).
- [9] V. Shiltsev, *et al.*, “Beam-Beam Effects in the Tevatron,” PRSTAB, **8**, 101001 (2005).
- [10] Y. Alexahin, “On the Landau Damping and Decoherence of Transverse Dipole Oscillations in Colliding Beams”, Part. Acc. **59**, 43 (1996)